



## Short communication

## Enhanced electro-oxidation of alcohols at electrochemically treated polycrystalline palladium surface



Lianqin Wang<sup>a,c</sup>, Manuela Bevilacqua<sup>a</sup>, Yan-Xin Chen<sup>a,c</sup>, Jonathan Filippi<sup>a</sup>,  
Massimo Innocenti<sup>a,b</sup>, Alessandro Lavacchi<sup>a,\*</sup>, Andrea Marchionni<sup>a</sup>, Hamish Miller<sup>a</sup>,  
Francesco Vizza<sup>a,\*</sup>

<sup>a</sup> Istituto di Chimica dei Composti Organometallici (ICCOM-CNR), National Research Council CNR, Via Madonna del Piano 10, 50019 Sesto Fiorentino, Italy

<sup>b</sup> Dipartimento di Chimica, Università di Firenze, Via della lastruccia 3, Sesto Fiorentino 50019, Italy

<sup>c</sup> University of Trieste, Via Licio Giorgieri, 1, Trieste 34127, Italy

## H I G H L I G H T S

- A facile activation protocol for polycrystalline Pd electrode is proposed.
- The protocol results in enhanced electro-catalytic activity toward alcohols oxidation.
- Activity enhancement is explained in terms of roughening and coordination of surface Pd atoms.

## A R T I C L E I N F O

## Article history:

Received 27 February 2013

Received in revised form

30 May 2013

Accepted 12 June 2013

Available online 20 June 2013

## Keywords:

Electrocatalysis

Palladium electrochemistry

Alcohols electro-oxidation

In situ FTIR spectroscopy

Direct alcohol fuel cells

## A B S T R A C T

The present study demonstrates the effectiveness of an electrochemical treatment consisting in cycles of constant potential oxidation and reduction of polycrystalline palladium surface in the enhancement of the electro-oxidation of ethanol, ethylene glycol and glycerol. The rise of the activity after the treatment has been ascribed to the increase of both surface area and density of low coordination surface atoms. FTIR spectra showed that a change in the reaction products distribution also occurs, resulting, in some cases, in an increased tendency to cleave the C–C bond.

© 2013 Elsevier B.V. All rights reserved.

## 1. Introduction

Direct alcohol fuel cells (DAFCs) are devices where the free energy of an alcohol can be converted into electrical energy, with contemporaneous release of higher added-value products. A crucial role for achieving this goal is played by the anode electrocatalysts that must promote the partial oxidation of renewable alcohols such as ethanol, glycerol, ethylene glycol, to carboxylic compounds, preferentially in a selective way and with fast kinetics.

We have shown that alcohols partial oxidation is particularly effective in alkaline electrolytes when using palladium as anode electrocatalyst. This finding has led to the development of platinum-free alkaline DAFCs [1–5]. Palladium-based anodes have also been applied to the electrolysis of hydro-alcoholic electrolyte, lowering the energy required for the H<sub>2</sub> production from alcohols [6].

High index palladium facets have been previously shown to be effective for small organic molecules oxidation [7]. A specifically designed redox treatment has been shown to further enhance the activity toward alcohols electro-oxidation with Pd nanoparticles deposited on TiO<sub>2</sub> nanotube arrays. The effect has been ascribed to the increase of the catalyst surface area and to the formation of high index facets [8]. Such a facile activation of palladium nanoparticles has been denoted as Electrochemical Milling and Faceting (ECMF)

\* Corresponding authors. Tel.: +39 0555225250; fax: +39 0555225203.

E-mail addresses: [alessandro.lavacchi@iccom.cnr.it](mailto:alessandro.lavacchi@iccom.cnr.it) (A. Lavacchi), [francesco.vizza@iccom.cnr.it](mailto:francesco.vizza@iccom.cnr.it) (F. Vizza).

for its ability to provoke mean particle size reduction together with an increase in the formation of high index faceted nanocrystals.

Here we report that an analogous treatment magnifies alcohols electro-oxidation at polycrystalline bulk palladium electrodes investigating the effect of the treatment on the oxidation of ethanol (E), ethylene glycol (EG) and glycerol (G). The choice of using E relied on its abundance and because of its use as a fuel for DAFC for portable devices power supply [14,9]. Further E oxidation in alkaline environment leads to the formation of acetate which is a valuable chemical process [1]. EG is a renewable product obtained from biomass feedstock and its oxidation also lead to the formation of valuable chemicals such as oxalate which is important in the synthesis of a variety of polymers [10] G is also extremely interesting as it is one of the major by-products of biodiesel production. At present its disposal is a major issue for the bio-fuel industry. G valorization through energy,  $H_2$  and chemical production would benefit the whole biodiesel production cycle, decreasing environmental impact, also benefitting economic and energy revenue [11]. G oxidation products are known to have wide industrial application e.g. pharmaceutical and cosmetic industry [12].

## 2. Material and methods

The working electrode consisted in a polycrystalline Pd disk ( $\Phi = 6$  mm) embedded in a Teflon cylinder. Pd electrode surface has been mechanically polished with polycrystalline diamond suspension with size down to  $1\ \mu\text{m}$  and than washed in a FALC sonic bath.

Electrochemical measurements have been performed with a PARSTAT 2273 potentiostat/galvanostat (Princeton Applied Research, USA) in a three-electrode cell arrangement at room temperature. An Ag/AgCl electrode has been used as reference, while counter-electrode consisted in a platinum wire (0.5 mm diameter). All the solutions have been purged with  $N_2$  for at least

$\frac{1}{2}$  h before any electrochemical experiment. All the reported potential have been quoted against the Reference Hydrogen Electrode (RHE) scale.

The Electrochemical (EC) treatment has been performed through potentiostatic oxidation and reduction cycles respectively at 4.55 V for oxidation (180 s) and  $-1.95$  V (vs. RHE) for reduction (180 s) respectively. The whole red-ox sequence has been repeated three times. All the Cyclic Voltammetry (CV) data have been determined until stabilization of the CV shape and current density has been obtained. Reported CV has been acquired at a scan rate of  $50\ \text{mV s}^{-1}$ . No iR-drop compensation has been applied.

Electrochemical in-situ FTIR reflection spectroscopy has been performed on a Nicolet 6700 spectrometer equipped with a DTGS detector. The spectro-electrochemical cell has been designed to have the Pd electrode supported by a  $\text{CaF}_2$  window. Such configuration allows only a thin film of electrolyte ( $10\ \mu\text{m}$  range) to be in the gap between the electrode and the window. Each infrared spectrum has been determined averaging 128 interferograms acquired with a resolution of  $4\ \text{cm}^{-1}$ . The reference spectrum ( $R_{\text{ref}}$ ) was collected at 0 V vs. RHE. Potential steps have been set to 0.1 V until 1.2 V has been reached. A spectrum has been normalized according to Equation (1) [13].

$$\frac{\Delta R}{R} = \frac{R_s - R_{\text{ref}}}{R_{\text{ref}}} \quad (1)$$

Under such a representation scheme, negative and positive bands correspond to produced and consumed species respectively.

## 3. Results and discussion

Alteration of the palladium electrode morphology has been demonstrated by SEM inspection of the electrode surface. Fig. 1a and b report the low and high magnification SEM images of the

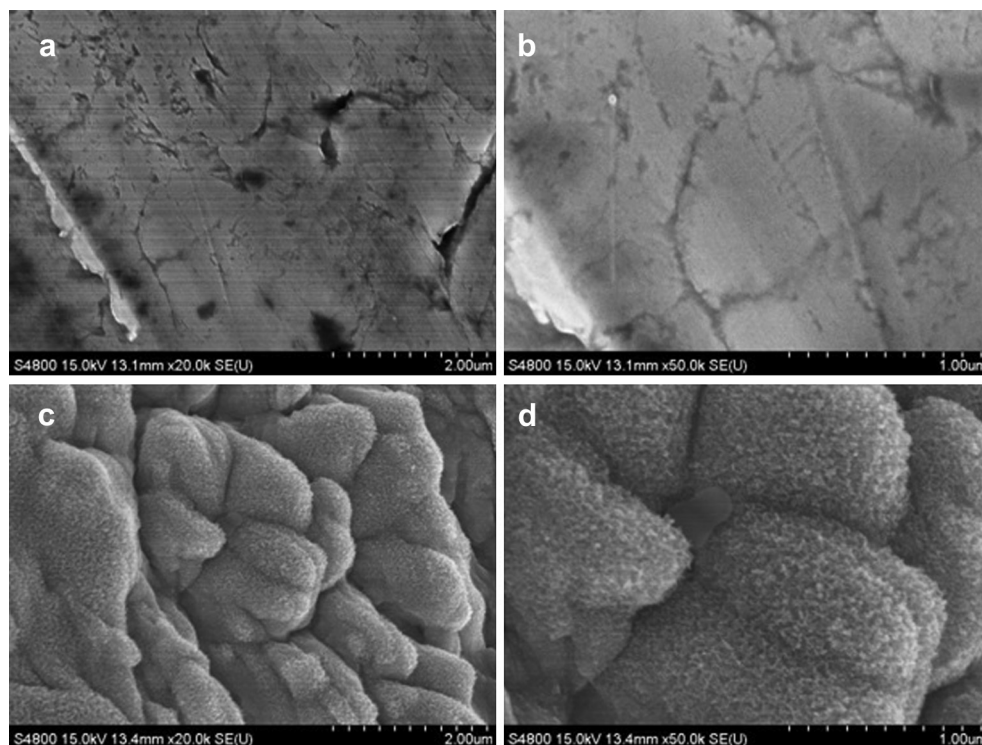


**Fig. 1.** Scanning Electron Microscopy images of Pd surfaces before (low magnification (a), high magnification (b)) and after the electrochemical treatment (low magnification (c), high magnification (d)).

polycrystalline Pd foil surface after polishing with 1  $\mu\text{m}$  diamond paste. Fig. 1c and d shows the low and high magnification SEM micrographs of the same surface after the EC treatment. Image comparison reveals dramatic surface roughening after treatment. Electrochemical roughening of polycrystalline palladium foil as a result of oxidation and reduction cycles has been previously observed and it has been exploited in the magnification of the Surface Enhanced Raman Scattering [14]. The extent of roughening has been quantified by the Electrochemically Active Surface Area (EASA) determination. EASA measurements have been performed by CV through the quantification of the cathodic peak corresponding to the reduction of a complete PdO monolayer (1.4 V vs. RHE according to what reported in Ref. [15]) in alkaline electrolyte. Table 1 shows that the EC treatment results in a twofold increase of the EASA. Fig. 2a reports the CV recorded in 2 M KOH before and after the treatment, showing that the reduction of PdO occurs between 0.6 V and 0.8 V. The shift of the CV toward more anodic currents after the EC treatment has been ascribed to the oxidation of hydrogen absorbed in Pd.

According to what previously reported [8], we recorded CVs in 0.1 M  $\text{HClO}_4$  to investigate oxygen adsorption/desorption electrochemical features before and after the treatment. We found a significant current density increase in the potential region between 0.6 and 0.8 V after the EC treatment which reveals an increase in the density of poorly coordinated palladium atoms. The origin of such increased density may be ascribed to the rise of the number of exposed high index facets, even if the formation of crystal defects, such as twins or stacking faults, may not be excluded.

The electrocatalytic activity toward the oxidation of alcohols (Fig. 2b–d) has been estimated by CV in 2 M KOH electrolytes containing 10 wt.% of E, and 5 wt.% of EG and G. Such conditions have been selected according to what reported, such fuel compositions have been found to be effective for powering alkaline DAFCs. We have found that the treated Pd electrode provides lower on-set potentials as compared to the non-treated ones for all the investigated electrolytes, also showing a dramatic increase of the peak current density for the alcohol oxidation (Table 1). The ratio between the CV current densities after and before the treatment resulted 5.6, 4.0 and 4.4 for the oxidation of E, EG and G, respectively. Such ratios are much larger than the ratio between the EASA after and before the treatment which, indeed, was 2.5. Thus, the EC treated Pd shows much higher activity toward alcohol electro-oxidation as compared to the non-treated Pd, and such an effect cannot be explained solely by surface roughening. According to CV performed in  $\text{HClO}_4$  and to what reported in the literature [8] we ascribed the activity enhancement to a convolution of effect due to the enlarged surface area and the increase in the density of poorly coordinated palladium atoms.

Alcohols electro-oxidation has also been investigated by in-situ FTIR spectroscopy. FTIR spectra reported in Fig. 3a and b and recorded in 2 M KOH containing ethanol wt.10% show four downward bands at 1550, 1415, 1346 and 1018  $\text{cm}^{-1}$  which can be safely assigned to  $\text{CH}_3\text{COO}^-$  [16,17]. Nevertheless it is known that the

**Table 1**  
Parameters for the catalytic activity assessment.

		Before EC treatment	After EC treatment
EASA ( $\text{cm}^2$ )		2.8	7.0
Onset potential (V vs. RHE)	Ethanol	0.39	0.19
	Ethylene glycol	0.50	0.37
	Glycerol	0.59	0.40
Peak current density/EACA peak current density ( $\text{mA cm}^{-2}$ )	Ethanol	34.4/3.5	193.9/7.8
	Ethylene glycol	52.4/5.3	207.3/8.4
	Glycerol	28.7/2.9	124.9/5.0

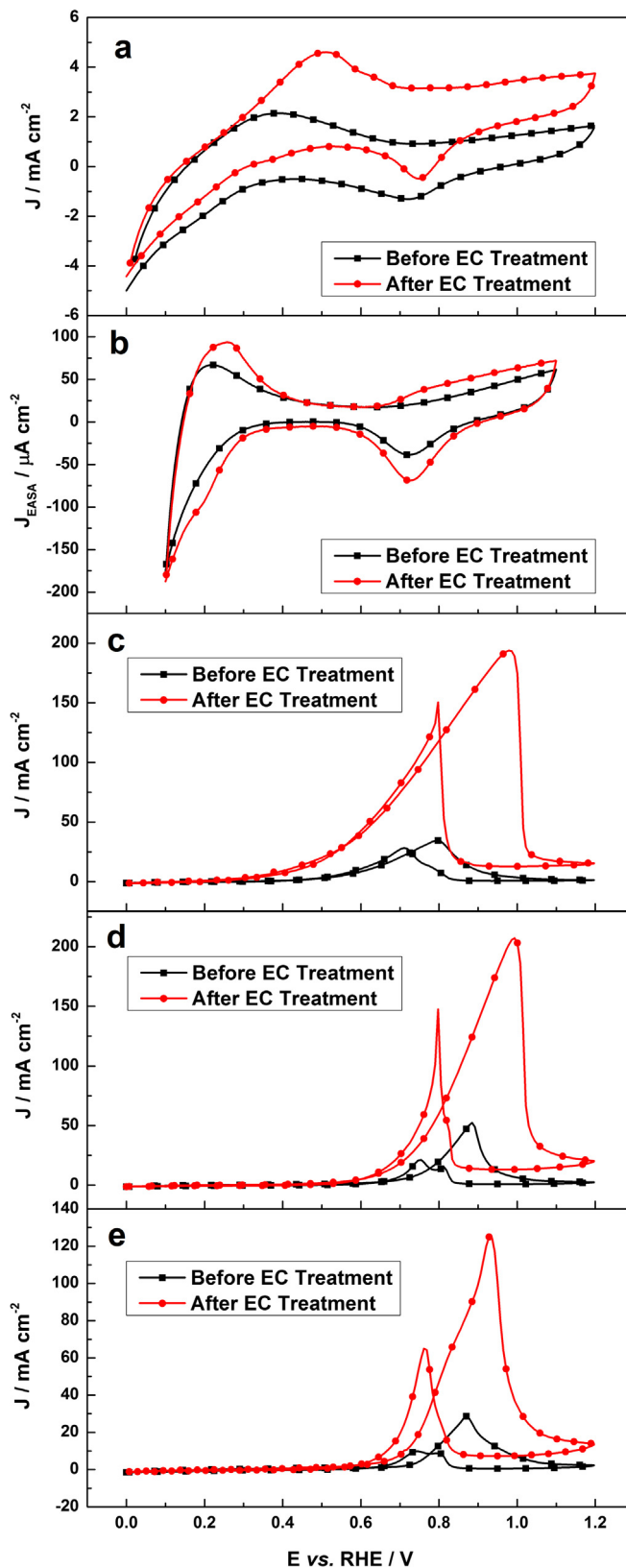


**Fig. 2.** Cyclic voltammograms of Pd in a) 2 M KOH; b) 0.1 M  $\text{HClO}_4$ ; c) 10 wt.% EtOH + 2 M KOH; d) 5 wt.% ethylene glycol + 2 M KOH; e) 5 wt.% glycerol + 2 M KOH. Scan rate: 50  $\text{mV s}^{-1}$ .

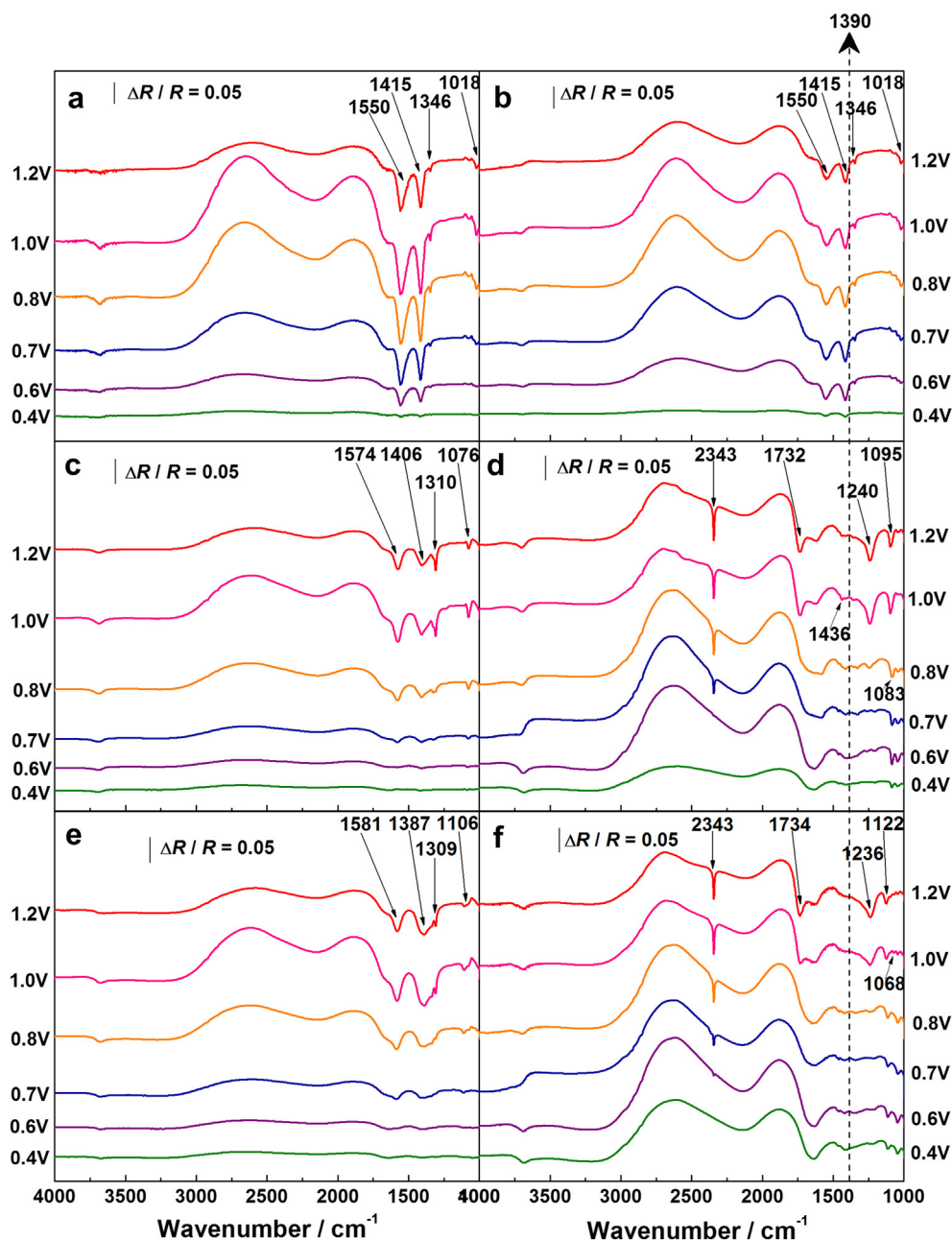


**Fig. 3.** In situ FTIR spectra obtained under potential step polarization in 10% ethanol + 2 M KOH on Pd a) before EC treatment and b) after EC treatment; in 5% ethylene glycol + 2 M KOH on Pd c) before EC treatment and d) after EC treatment; in 5% glycerol + 2 M KOH on Pd e) before EC treatment and f) after EC treatment.

symmetric stretching of  $\text{COO}^-$  ( $1415\text{ cm}^{-1}$ ) is less intense than the asymmetric stretching band occurring at  $1550\text{ cm}^{-1}$  [16]. This is not the case of the spectrum reported in Fig. 3b. Indeed here the band intensity at  $1415\text{ cm}^{-1}$  is significantly larger as compared to the band at  $1550\text{ cm}^{-1}$ . This effect has been described elsewhere [16] and has been ascribed to the formation of carbonate resulting in the rise of a band with peak at  $1390\text{ cm}^{-1}$ . Such a band cannot be fully resolved from the  $1415\text{ cm}^{-1}$  acetate signal. This evidence may indicate a larger tendency of the EC treated surfaces to produce C–C cleavage. It is known that differences in the distribution of the surface sites (terraces, steps and kinks) results in variation of the selectivity of the oxidation products. Such an effect has been proved to be effective for enhancing the electrochemical cleavage of the ethanol C–C on high index faceted Pt [18]. The change may also be

due to local change in the pH for the larger activity of the system after EC treatment. Local variations of the pH in spectroelectrochemical experiments with thin film cells have been previously observed [16,19–21] and their effect cannot be excluded here. Furthermore reduction in pH has been observed to increase the extent of the C–C cleavage in ethanol electrooxidation [17].

At potential lower than 0.7 V for EG before the EC treatment we obtained oxidation bands with very low intensity, not allowing a safe assignment. At potential of 0.7 V and higher we observe the formation of mixed carboxylates such as glycolate ( $1574\text{ cm}^{-1}$  and  $1406\text{ cm}^{-1}$ ) [22] and oxalate ( $1570\text{ cm}^{-1}$  and  $1310\text{ cm}^{-1}$ ) [23,24]. Further the formation of  $\text{CO}_3^{2-}$  cannot be excluded due to the superimposition of the carbonate bands to that of carboxylates. The electrooxidation of the EC treated sample at potential higher than



0.7 V leads to the formation of glycolic acid ( $1732\text{ cm}^{-1}$ ,  $1436\text{ cm}^{-1}$ ,  $1083\text{ cm}^{-1}$ ), oxalic acid ( $1732\text{ cm}^{-1}$ ,  $1240\text{ cm}^{-1}$ ), glyoxylic acid ( $1736\text{ cm}^{-1}$ ,  $1240\text{ cm}^{-1}$ ,  $1095\text{ cm}^{-1}$ ) and glyoxal ( $1415\text{ cm}^{-1}$ ,  $1083\text{ cm}^{-1}$ ) [24–26].

The electro-oxidation of G before the EC treatment resulted in the formation of glycerate ( $1581\text{ cm}^{-1}$ ,  $1387\text{ cm}^{-1}$  and  $1309\text{ cm}^{-1}$ ) [27] for potential higher than 0.7 V. Carbonate formation cannot be excluded for the superimposition of the  $\text{COO}^-$  symmetric stretching band of glycerate with that of carbonate. Instead, after the treatment, the formation of mixed carboxylic acids at potentials higher than 0.6 V has been detected together with  $\text{CO}_2$  ( $2343\text{ cm}^{-1}$ ) formation.

Both for the EG and G electro-oxidation (Fig. 2d, f) the presence of carboxylic acids and  $\text{CO}_2$  instead of carboxylates and carbonate suggests pH decrease in the probed thin layer solution. pH decrease originates from the  $\text{OH}^-$  consumption in the alcohols oxidation reaction. The phenomenon resulted more pronounced in the case of the EC treated surface for the much higher catalytic activity as compared with the non treated one. In the end FT-IR data not only support the CV evidence for the increase in the electrocatalytic activity after EC treatment, but also may suggest differences in the reactivity.

#### 4. Conclusion

We have demonstrated that constant potential oxidation reduction cycles enhance the electrocatalytic activity of polycrystalline palladium surfaces toward alcohols electro-oxidation. The investigation revealed that the increase in the catalytic activity has to be explained accounting for both a dramatic increase in the surface and an increase in the specific activity. The reason for the latter has been ascribed to the rise of the density of low coordination palladium atoms which are known to better catalyze small organic molecules oxidation. Such findings lead to the proposition of our treatment as an activation protocol for palladium surfaces. Such treatment may lead to improvement in the efficiency of platinum free alkaline DAFC as well as to the optimization of

electrolytic processes for the simultaneous production of hydrogen and valuable chemicals.

#### Acknowledgments

MSE for the PRIT project Industria 2015; the MIUR (Italy) for the FIRB 2010 project RBFR10J4H7\_002.

#### References

- [1] C. Bianchini, P.K. Shen, *Chem. Rev.* 109 (2009) 4183.
- [2] L. Wang, V. Bambagioni, M. Bevilacqua, C. Bianchini, J. Filippi, A. Lavacchi, A. Marchionni, F. Vizza, X. Fang, P.K. Shen, *J. Power Sources* 195 (2010) 8036.
- [3] V. Bambagioni, C. Bianchini, J. Filippi, W. Oberhauser, A. Marchionni, F. Vizza, R. Psaro, L. Sordelli, M.L. Foresti, M. Innocenti, *ChemSusChem* 2 (2009) 99.
- [4] E. Antolini, E.R. Gonzalez, *J. Power Sources* 195 (2010) 3431.
- [5] E. Antolini, *Energy Environ. Sci.* 2 (2009) 915.
- [6] V. Bambagioni, M. Bevilacqua, C. Bianchini, J. Filippi, A. Lavacchi, A. Marchionni, F. Vizza, P.K. Shen, *ChemSusChem* 3 (2010) 851.
- [7] N. Tian, Z.Y. Zhou, N.F. Yu, L.Y. Wang, S.G. Sun, *J. Am. Chem. Soc.* 132 (2010) 7580.
- [8] Y.X. Chen, A. Lavacchi, S.P. Chen, F. Benedetto, M. Bevilacqua, C. Bianchini, P. Fornasiero, M. Innocenti, M. Marelli, W. Oberhauser, S.G. Sun, F. Vizza, *Angew. Chem. Int. Ed.* 51 (2012) 1.
- [9] M.R. Schmer, K.P. Vogel, R.B. Mitchell, R.K. Perrin, *Natl. Acad. Sci.* 105 (2008) 464.
- [10] N. Ji, T. Zhang, M.Y. Zheng, A.Q. Wang, H. Wang, X.D. Wang, J.G. Chen, *Angew. Chem. Int. Ed.* 120 (2008) 8638.
- [11] S. Miele, E. Bargiacchi, *Chim. Oggi* 26 (2008) 30.
- [12] M. Simões, S. Baranton, C. Coutanceau, *ChemSusChem* 5 (2012) 2106.
- [13] K. Ashley, *Chem. Rev.* 88 (1988) 673.
- [14] Z. Liu, Z.-L. Yang, L. Cui, B. Ren, Z.-Q. Tian, *J. Phys. Chem. C* 111 (2007) 1770.
- [15] M. Grdeń, M. Łukaszewski, G. Jerkiewicz, A. Czerwiński, *Electrochim. Acta* 53 (2008) 7583.
- [16] Z.Y. Zhou, Q. Wang, J.L. Lin, N. Tian, S.G. Sun, *Electrochim. Acta* 55 (2010) 7995.
- [17] X. Fang, L.Q. Wang, P.K. Shen, G.F. Cui, C. Bianchini, *J. Power Sources* 195 (2010) 1375.
- [18] N. Tian, Z.-Y. Zhou, S.-G. Sun, *J. Phys. Chem. C* 112 (2008) 19801.
- [19] T. Iwasita, F.C. Nart, *Prog. Surf. Sci.* 55 (1997) 271.
- [20] R.S. Ferreira Jr., M.J. Giz, G.A. Camara, *J. Electroanal. Chem.* 697 (2013) 15.
- [21] L. Wang, H. Meng, P.K. Shen, C. Bianchini, F. Vizza, Z. Wei, *Phys. Chem. Chem. Phys.* 13 (2011) 2667.
- [22] S.E. Cabaniss, I.F. McVey, *Spectrochim. Acta Part A* 51 (1995) 2385.
- [23] T.J. Strathmann, S.C.B. Myneni, *Geochim. Cosmochim. Acta* 68 (2004) 3441.
- [24] S.E. Cabaniss, J.A. Leenheer, I.F. McVey, *Spectrochim. Acta Part A* 54 (1998) 449.
- [25] A. Falase, M. Main, K. Garcia, A. Serov, C. Lau, P. Atanassov, *Electrochim. Acta* 66 (2012) 295.
- [26] A. Falase, K. Garcia, C. Lau, P. Atanassov, *Electrochem. Commun.* 13 (2011) 1488.
- [27] M. Simões, S. Baranton, C. Coutanceau, *Appl. Catal. B Environ.* 93 (2010) 354.